Effects of SWBLI and SWSWI in Mars Atmosphere Entry

Gennaro Zuppardi

Department of Industrial Engineering – Aerospace Division
University of Naples "Federico II", Piazzale Tecchio 80, 80125 Naples, Italy

zuppardi@unina.it

Abstract. The forthcoming manned exploration missions to Mars by means of complex geometry spacecrafts stimulate the study of aerodynamic, hypersonic phenomena such as Shock Wave-Boundary Layer Interaction (SWBLI) and Shock Wave-Shock Wave Interaction (SWSWI) also along the entry in Mars atmosphere. As already done by Zuppardi and co-workers in early papers where SWBLI and SWSWI were studied in Earth re-entry, also the present study has been carried out computationally by means of a DSMC code. The aim of the present paper is to quantify the effects of SWBLI and of SWSWI at the conditions of Mars entry and to compare these effects with those, already computed by the author at the conditions of Earth re-entry. Also in this paper, SWBLI has been studied considering an external, oblique shock wave impinging onto a flat plate on which gas was flowing and therefore a boundary layer was present. Computations have been carried out in the altitude interval 55-70 km. SWSWI has been studied considering the interaction of the shock wave on the leading edge of an airfoil (NACA-0010) with the shock wave stemming from the airfoil concave, lower surface at the hinge position in flapped configuration. Computer tests have been carried out at the altitude of 65 km, in the range of angles of attack 0-40 deg and considering three flap deflections: 0, 15, 30 deg. The quantification of the effects of both interactions has been carried out by means of the relative increase of local quantities such as the resultant of pressure, normal and tangential stresses and the heat flux. SWSWI has been quantified also in terms of global aerodynamic coefficients. The analysis verified that the SWBLI effects are higher in Earth re-entry. SWSWI is also higher in Earth re-entry in terms of global coefficients but the effects are higher in Mars entry in terms of the relative increase of local quantities.

INTRODUCTION

The forthcoming manned exploration missions to Mars by means of complex geometry spacecrafts, as per lifting vehicles provided with control aerodynamic surfaces like wing-flaps, body-flaps, elevons, etc., stimulate the study of aerodynamic, hypersonic phenomena that could occur in Earth re-entry, such as Shock Wave-Boundary Layer Interaction (SWBLI) and Shock Wave-Shock Wave Interaction (SWSWI) also along the entry in Mars atmosphere.

SWBLI and SWSWI are strongly unwanted; both ones should be avoided because involving consistent increases of pressure, normal and tangential stresses and heat flux on the spacecraft surface. Thus, the surface should be equipped with a mechanical and Thermal Protection System (TPS). Besides these drawbacks, SWSWI is also important because of the effects on the spacecraft global aerodynamic coefficients. The aim of the present work is to quantify the effects of SWBLI and of SWSWI at the conditions of Mars entry and to compare these effects with those, already computed by Zuppardi [1-4], at the same altitudes in Earth re-entry.

SWBLI was studied considering the impingement of an external, oblique shock wave onto a flat plate [1] on which air was flowing and therefore a boundary layer was present. SWSWI was studied considering the interaction of an oblique shock wave impinging onto the bow shock wave on a circular cylinder [2]. More specifically, the Edney's "type IV" SWSWI was analyzed. This type of interaction produces, in fact, the most severe increments of pressure and heat flux on the body surface. This interaction was studied also considering the oblique shock wave coming from the leading edge of an airfoil with the shock wave stemming from the hinge position on the concave, lower surface of flapped airfoil [3, 4].

In order to make comparable the present results with those already obtained for Earth, also in the present paper: 1) SWBLI is studied considering that the oblique shock wave, impinging onto a flat plate, is produced by the same wedge (20 deg) used in Earth computations, 2) SWSWI is studied considering the same airfoil (NACA-0010) in the same interval of angles of attack (0-40 deg), the same extension (35% of the chord) of the trailing edge flap and the same deflection angles (0, 15, 30 deg). The effects of both interactions are quantified by means of the relative increase of local quantities such as the resultant of pressure, normal and tangential stresses and the heat flux on the body surface and of global aerodynamic coefficients with respect to the same quantities with no shock wave interaction.

Once again, both interactions are studied computationally by means of the Direct Simulation Monte Carlo code DS2V-4.5 64 bits [5]. Even though, as shown later, the rarefaction level of the flow fields involved in this study, is such that the flow fields could be solved also by means of a Navier-Stokes code, however a DSMC code has been

preferred because the complexity of the flow fields in the interaction regions could produce problems to a Navier-Stokes code.

PHYSICS OF SWBLI AND SWSWI

Physics and basic phenomena of SWBLI are widely described by Anderson [6], those of SWSWI by Bertin [7]. The description of both interactions has been also summarized by Zuppardi in [1] and in [3], respectively and here resumed for the sake of completeness.

The impingement of a shock wave onto a boundary layer (SWBLI) produces abrupt increases of temperature and of pressure. The increase of pressure across the impinging shock wave works like an adverse pressure gradient, leading to a local boundary layer separation upstream the impingement point (Fig.1(a)). Flow reattaches to surface, forming a separation bubble. The separation bubble produces, in turn, an oblique shock wave called "induced separation shock". An expansion fan, downstream the induced separation shock, turns the flow toward the surface. A shock wave, called "reattachment shock", departs from the reattachment point. The "induced separation shock" and the "reattachment shock" merge at some distance from the surface, forming the conventional "reflected shock". The reflected shock wave produces, on the underlying surface, values of pressure, skin friction and heat flux higher than those with no interaction.

The separation bubble can be detected by a decrease of heat flux and of tangential stress as well as by a plateau of pressure. The tangential stress can plummet to zero and even change sign in the bubble. When flow reattaches, pressure, skin friction and heat flux increase up to a relative maximum; the relative maximum indicates the completion of the reattachment process. After this point, the trends of these quantities are similar to those with no interaction; the interaction region can be considered finished when a generic quantity takes values comparable with those without shock wave impingement.

SWSWI, considered in the present work, is produced by the interaction of two oblique shock waves of the same family. As already pointed out before, in the present study a shock wave is produced by the airfoil leading edge, the other shock wave comes from the hinge position on the concave, lower surface of the same flapped airfoil. Figure 1(b) provides a scheme of what said; the interacting waves are labeled A and B. The shock waves are of the same family but of different slopes, thus they can merge at some distance from the surface. The shock wave generated by interaction is labeled as C. The point where the shock waves interact, called "triple point", is labeled as I.

A slip line originates from point I. This slip line separates the flow field in two regions labeled as 4 and 6. In region 4, the flow passes through the two shock waves A and B. In region 6, the flow passes through the single shock wave C. Thus, the pressure should be higher in 4 than in 6. In order to decrease the pressure in 4 and therefore to restore equilibrium of the slip line, an expansion fan generates from point I. This fan impinges onto the body surface and reflects again as an expansion fan. Despite the presence of two systems of expansion waves, the shock wave C increases pressure and temperature to values higher than those without SWSWI in the part of the flow field labeled as 5, hence on the underlying body surface.

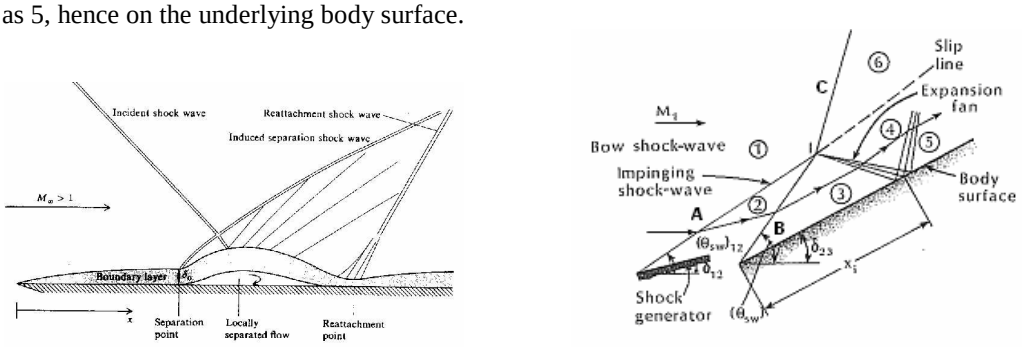

FIGURE 1. Sketches of: (a) Shock Wave-Boundary Layer Interaction (from Anderson [6]), (b) Shock Wave-Shock Wave Interaction (from Bertin [7])

DIRECT SIMULATION MONTE CARLO METHOD AND DS2V-4.5 64 BITS CODE

It is well known that the Direct Simulation Monte Carlo (DSMC) method [8, 9, 10] is currently the only available tool for the solution of rarefied flow fields from continuum low density regime (or slip flow) to free molecular regime. DSMC considers a gas as made up of discrete molecules; it is based on the kinetic theory of gases and computes the evolution of millions of simulated molecules, each one representing a large number of real molecules in the physical space, for example, in the present computations between 10^{14} and 10^{15}. Molecule-molecule collisions and molecule-surface interactions are computed. The computation domain is divided into cells, used both for selecting the colliding molecules and for sampling the macroscopic, fluid-dynamic quantities. The most important advantage of the method is that it does not suffer from numerical instabilities and does not directly rely on similarity

parameters (i.e. Mach and Reynolds numbers). However, it is inherently unsteady; a steady solution is achieved after a sufficiently long simulated time.

The DSMC code, used in the present study, is the 2-D/axial-symmetric DS2V-4.5 64 bits code [5]. This code is "sophisticated". As widely reported in literature [11, 12, 13], a DSMC code is defined sophisticated if it implements computing procedures providing higher efficiency and accuracy with respect to a "basic" DSMC code. A sophisticated code, in fact, considers two sets of cells (collision and sampling) with the related cell adaptation and implements methods promoting "nearest neighbour" collisions. This type of code generates automatically computation parameters such as numbers of cells and of simulated molecules by the input numbers of megabytes and of the free stream number density. It uses a "radial weighting factor" routine in solving axial-symmetric flow fields and provides optimal time step. Finally, the same collision pair cannot have sequential collisions.

Besides being sophisticated, DS2V-4.5 64 bits is also advanced; the user can verify that the numbers of simulated molecules and of collision cells are adequate by means of the on line visualization of the ratio between the molecule mean collision separation (mcs) and the local mean free path (λ) in each collision cell. In addition, the code allows the user to change (or to increase), during a computation, the number of simulated molecules. The ratio mcs/λ has to be less than unity everywhere in the computation domain for an acceptable quality of the results. Bird [11] suggests 0.2 as a limit value for an optimal quality of the results. In addition, the code gives the user information about the stabilization of a computation by means of the profile of the number of simulated molecules as a function of the simulated time. According to Bird [11], the stabilization of a DSMC calculation is achieved when this profile becomes jagged and included within a band defining the standard deviation.

TEST CONDITIONS

For Mars computations, the free stream velocity is that of a non-lifting capsule during free entry in the altitude interval 55-70 km [14]. Unfortunately, at knowledge of the author, the Mars entry trajectory of a winged space vehicle, such as it should have been, is not jet available. The Mars atmosphere parameters are computed by means of the NASA Glenn Research Center model. For the purpose of the present paper, the chemical model of the Mars atmosphere used by Bird in the previous version 3.3 of the DS2V code [15], has been implemented in the current version of the code. This model considers the Mars atmosphere as made up of 9 species with molar fractions X_{O2}=0.00176, X_{N2}=0.04173, X_{NO}=0.00014, X_{C}=0.00396, X_{CO}=0.00108, X_{CO2}=0.93399, X_{AR}=0.01734, constant with altitude and relies on 54 chemical reactions.

The free stream velocity for Earth computations was that of the Italian aero-space-plane Flight Test Bed FTB-X [16] during the re-entry in the same altitude interval. The Earth atmosphere parameters and the gas composition were provided by the US Standard Atmosphere 1976. Also for Earth, the atmosphere composition is almost constant in the altitude interval 55-70 km: $X_{O2}\cong 0.21$, $X_{N2}\cong 0.79$. Tables 1(a) and 1(b) report the input data (V_∞, N_∞, T_∞) to DS2V-4.5 64 bits for Mars and for Earth, respectively (the latter already used for the computations made in [1]) and some aerodynamic parameters for the characterization of the flow fields.

TABLE 1(a). DS2V-4.5 64 bits input data and some aerodynamic parameters: Mars

h [km]	V_∞ [m/s]	N_∞ [1/m^3]	T_∞ [K]	ρ_∞ [kg/m^3]	$\rho_\infty V^2_\infty$ [N/m^2]	$\rho_\infty V^3_\infty$ [W/m^2]	M_∞	$Re_{L=1\infty}$	$Kn_{L=1\infty}$
70	4374	9.86×10^{20}	94	7.09×10^{-5}	1.36×10^{3}	0.59×10^{7}	28.4	6.15×10^{4}	6.09×10^{-4}
65	4235	1.38×10^{21}	105	9.94×10^{-5}	1.74×10^{3}	0.76×10^{7}	26.1	7.54×10^{4}	4.55×10^{-4}
60	4044	1.96×10^{21}	117	1.41×10^{-4}	2.31×10^{3}	0.93×10^{7}	23.7	9.30×10^{4}	3.35×10^{-4}
55	3785	2.81×10^{21}	128	2.02×10^{-4}	2.89×10^{3}	1.10×10^{7}	21.2	1.14×10^{5}	2.43×10^{-4}

TABLE 1(b). DS2V-4.5 64 bits input data and some aerodynamic parameters: Earth

h [km]	V_∞ [m/s]	N_∞ [1/m^3]	T_∞ [K]	ρ_∞ [kg/m^3]	$\rho_\infty V^2_\infty$ [N/m^2]	$\rho_\infty V^3_\infty$ [W/m^2]	M_∞	$Re_{L=1\infty}$	$Kn_{L=1\infty}$
70	5933	1.72×10^{21}	220	8.20×10^{-5}	2.89×10^{3}	1.71×10^{7}	19.9	3.37×10^{4}	8.40×10^{-4}
65	5163	3.39×10^{21}	233	1.62×10^{-4}	4.32×10^{3}	2.23×10^{7}	16.8	5.51×10^{4}	4.32×10^{-4}
60	4624	6.44×10^{21}	247	3.07×10^{-4}	6.56×10^{3}	3.04×10^{7}	14.6	8.94×10^{4}	2.31×10^{-4}
55	4007	1.18×10^{22}	261	5.63×10^{-4}	9.04×10^{3}	3.62×10^{7}	12.3	1.36×10^{5}	1.28×10^{-4}

The Mars and the Earth free stream Knudsen numbers, based on a length of one meter ($Kn_{L=1\infty}$), verify that the rarefaction levels are pretty close. The Knudsen numbers indicate that the flow fields are in continuum low density regime. According to Moss [17], a general definition of the transitional regime, in terms of the Knudsen number ($Kn_{L=1\infty}$), is: $10^{-3}<Kn_{L\infty}<50$. For the sake of completeness, tables 1(a) and 1(b) report also the free stream Mach number (M_∞) and Reynolds number based on a length of one meter ($Re_{L=1\infty}$). The free stream dynamic pressure ($\rho_\infty V^2_\infty$) and energy flux ($\rho_\infty V^3_\infty$) are also reported. These quantities are meaningful because representative of the

aerodynamic and thermal loads, respectively. Both quantities for Earth are about three times greater than those for Mars.

The computation domain for SWBLI is a rectangle: L_x=5.0 m, L_y=0.6 m. Each horizontal side of the rectangle simulates a flat plate. The shock waves, impinging onto the flat plates, are generated by a 20 deg wedge, located at y=0.30 m from the two flat plates.

A NACA-0010 airfoil in clean and flapped configurations has been considered for the SWSWI computations. Figs. 2(a), 2(b) and 2(c) show the airfoil in "clean" configuration (δ=0 deg) and with the two flap angles of δ=15 deg and δ=30 deg, respectively. The airfoil chord (c) was 2 m and the flap hinge was located at 65% of the chord or at x=1.30 m. The airfoil surface was approximated by 1000 flat panels (500 on the lower surface and 500 on the upper surface). The computation domain was a rectangle: L_x=2.5 m, L_y=1.1 m. In both SWBLI and SWSWI computations, the surface was considered not-reactive and reflecting molecules diffusively at constant temperature of 300 K.

(a) (b) (c)

FIGURE 2. NACA-0010 airfoil with: δ=0 deg (a), 15 deg (b), δ=30 deg(c)

COMPUTATION PARAMETERS AND QUALITY OF THE RESULTS

The analysis for Mars relies on 35 computations: 8 for SWBLI (4 altitudes, with and without shock wave interaction) and 27 for SWSWI (9 angles of attack between 0-40 deg with a spacing of 5 deg and three flap deflections: 0, 15 and 30 deg) at the altitude of 65 km. The analysis for Earth relies on the results already obtained in [1] and [3]. Some parameters of the present computations are reported in tables 2(a) and 2(b) for the two kinds of interaction: number of simulated molecules (N_m), number of collision (N_C) and sampling (N_S) cells, number of molecule-surface interactions (N_I), number of real molecules represented by each simulated molecule (F_N), ratio mcs/λ, averaged over the computation domain, ratio t_s/t_f. t_s is the simulation time, t_f is the required time to travel the length L_X of the computation domain at the free stream velocity. The longer t_s, the larger the sample size over which the fluid-dynamic quantities are averaged during the evolution toward the steady state condition. Increasing the sample size, for making an average of the molecular properties, is equivalent to making a calculation with a larger number of molecules. Therefore, achieving the one to one correspondence between real and simulated molecules could be possible. If so, the fluid-dynamic fluctuations match those in the real gas. Furthermore, jagging of the profile of the number of simulated molecules versus the simulated time has been achieved in each computation.

Tables 2(a) and 2(b) report the above mentioned parameters at the most severe conditions of h=55 km for SWBLI and α=40 deg, δ=30 deg for SWSWI. Even though mcs/λ does not satisfy the optimal limit value of 0.2, however it is less than unit, as required by the DSMC method. On the other hand, the ratio t_s/t_f certainly satisfies the criterion of the stabilization of an unsteady, fluid-dynamic computation. In fact, a rule of thumb suggests considering a computation stabilized when the ratio t_s/t_f is O(10).

TABLE 2(a). DS2V-4.5 64 bits computation parameters for SWBLI: h=55 km

N_m	N_C	N_S	N_I	F_N	mcs/λ	t_s/t_f
3.26×10^7	1.23×10^6	9.32×10^4	1.23×10^8	2.85×10^{14}	0.710	2.50

TABLE 2(b). DS2V-4.5 64 bits computation parameters for SWSWI: h=65 km, α=40 deg, δ=30 deg

N_m	N_C	N_S	N_I	F_N	mcs/λ	t_s/t_f
2.76×10^7	2.98×10^6	1.06×10^5	1.57×10^8	3.02×10^{14}	0.689	2.15

ANALYSIS OF RESULTS

Shock Wave Boundary Layer Interaction: SWBLI

Figures 3(a), 3(b) and 3(c) show the profiles of: skin friction (τ), resultant (f) of pressure (p), normal stress (σ) and skin friction ($f=\sqrt{(p+\sigma)^2+\tau^2}$), heat flux ($\dot{q}$) along a flat plate with and without SWBLI at h=70 km. As already pointed out in [1], SWBLI influences heat flux, tangential stress, pressure and so on in different way, thus the evaluation of the extension of the interaction region can be slightly different, depending on the quantity utilized.

In the earlier [1] and in the present computations, the identification of the interaction region relies on the skin friction profile. The beginning of the separation bubble (x_B) is identified, in a clear way, by a decrease of τ. The interaction region is the zone on the surface between x_B and the point x_E where the shear stress profile takes the trend it should have without SWBLI; the length of the interaction region is $L_I=x_E-x_B$. Point x_R identifies a relative maximum of the profile of each quantity. As said before, this is the point where the flow reattachment completes. See the profile of τ for Earth in Fig.3(a) for visualizing x_B, x_R and x_E.

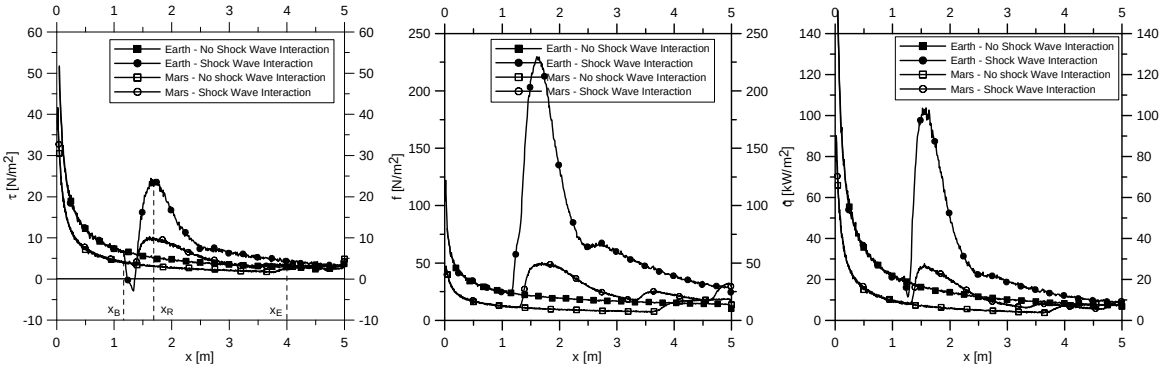

(a) (b) (c)

FIGURE 3. Profiles of skin friction (a), resultant stress (b), heat flux (c) along a flat plate: h=70 km

Figures 3(a), 3(b) and 3(c) show that SWBLI is stronger for Earth. This could be expected because, as reported in tables 1(a) and 1(b), both the dynamic pressure ($\rho_\infty V_\infty^2$) and the energy flux ($\rho_\infty V_\infty^3$) are higher for Earth. For Mars at h=70 km, the shock wave intensity is not strong enough to provoke a consistent inversion of the flow and therefore of the sign of τ. At this altitude, the maximum values of f and $\dot{q}$ for Earth are about 4.5 and 3.8 greater than those for Mars.

Table 3 quantifies, at each altitude, the intensity of SWBLI by the relative increments of the resultant stress ($\Delta f/f$) and of heat flux ($\Delta\dot{q}/\dot{q}$). These are computed as the differences between the maximum values of f and $\dot{q}$ with the values computed at the same points without interaction. Also $\Delta f/f$ and $\Delta\dot{q}/\dot{q}$ indicate that SWBLI for Earth is stronger than that for Mars. On the opposite, the lengths of the interaction regions are almost the same; $L_I \cong 2.5$ m.

TABLE 3. Comparison of the SWBLI effects for Mars and Earth

h [km]	Δf/f - Mars	Δf/f - Earth	Δq̇/q̇ - Mars	Δq̇/q̇ - Earth
70	3.9	9.8	2.8	5.3
65	4.4	12.2	2.8	6.7
60	5.2	14.9	3.6	9.3
55	5.3	15.7	3.5	9.2

Neumann [18], [6] found a formula linking the heat flux rise to the pressure rise in SWBLI:

$$\frac{\dot{q}_{max}}{\dot{q}_{NOSWBLI}} = \left(\frac{p_{max}}{p_{NOSWBLI}}\right)^n$$

where: n=0.5 for laminar flow, n=0.8 for turbulent flow. The good match of the present results (Fig.4) with those from the Neumann formula for turbulent flow indicates that the condition of turbulent flow holds also for Mars.

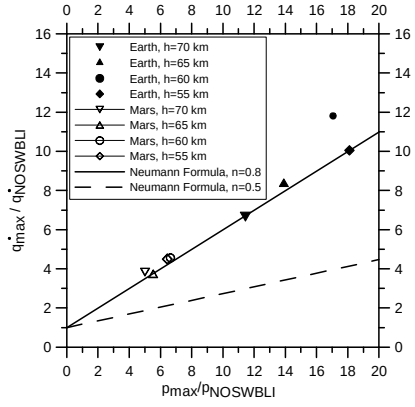

FIGURE 4. Correlation of the pressure rise to the heat flux rise in SWBLI

Shock Wave Shock Wave Interaction: SWSWI

The SWSWI effects can be qualitatively compared by means of Figs.5(a) to 5(d) where the 2-D maps of pressure and temperature in the flow field around the airfoil are reported for Earth (a), (c) and for Mars (b), (d) at: h=65 km, α=40 deg, δ=15 deg. For the sake of completeness, the streamline patterns are also drawn on the pressure maps. As expected, the lower values of the free stream dynamic pressure and of the energy flux for Mars produce, in the part of the flow field corresponding to the airfoil lower surface, lower pressure and lower temperature compared

with those computed for Earth. The free stream dynamic pressure and energy flux influence, in turn, also the profiles of the resultant stress and of heat flux on the airfoil lower surface (see Figs.6(a) and 6(b)). The profiles of the same quantities, computed in clean configuration, are also plotted in the same figures. The maximum values of f and $\dot{q}$ for Earth are about 1.7 and 1.4 times greater than those for Mars. But, unlike what seen for SWBLI, the relative increases $\Delta f/f$ and $\Delta\dot{q}/\dot{q}$ indicate that the SWSWI effects, for both flap angles, are higher for Mars (see table 4).

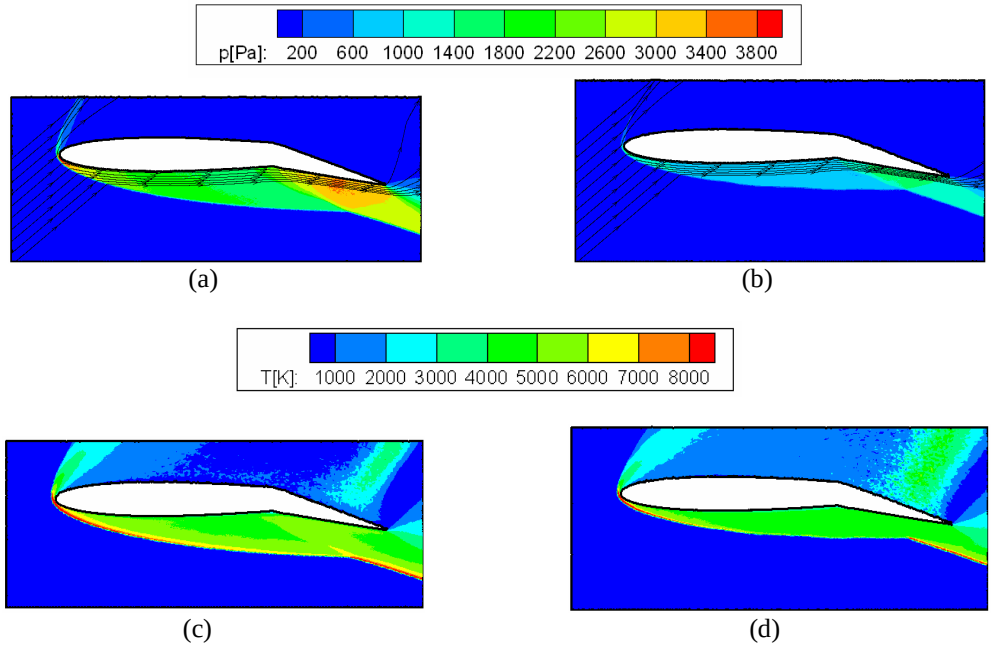

FIGURE 5. 2-D map of pressure and stream lines around the airfoil for Earth (a) and for Mars (b) and of temperature for Earth (c) and for Mars (d): h=65 km, α=40 deg, δ=15 deg

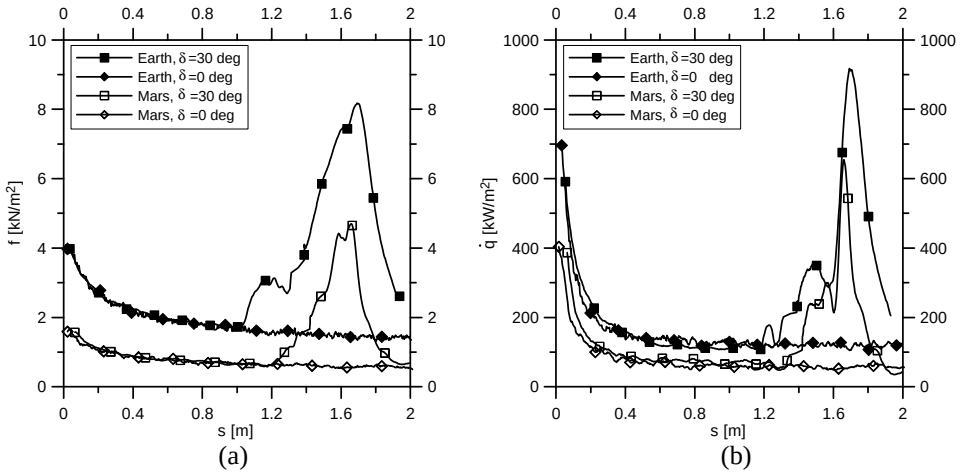

FIGURE 6. Profiles of resultant stress (a) and heat flux (b) along the airfoil lower surface for Earth and for Mars: h=65 km, α=40 deg

TABLE 4. Comparison of the SWSWI effects for Mars and Earth: h=65 km, α=40 deg

δ [deg	**Δf/f - Mars**	**Δf/f - Earth**	**$\Delta\dot{q}/\dot{q}$ - Mars**	**$\Delta\dot{q}/\dot{q}$ - Earth**
15	2.0	1.4	2.2	0.8
30	7.5	4.7	11.3	7.5

Figures 7(a) to 7(d) compare the profiles of the lift (a), drag (b), pitching moment coefficients (the reduction pole is the leading edge, c) and of the aerodynamic efficiency ($E=C_l/C_d$, d) as functions of the angle of attack, for Mars and for Earth. Figures show that the Earth and the Mars coefficients are comparable in the whole range of angles of attack for the airfoil in clean and δ=15 deg flapped configurations. The coefficients are comparable also with δ=30

deg at low angles of attack (roughly up to 10÷15 deg); this is due to negligible SWSWI effects. At higher angles of attach, the higher intensity of SWSWI influences the components of the aerodynamic force and therefore the related coefficients. Table 5 reports the relative variations of the lift, drag, pitching moment coefficients and of the aerodynamic efficiency, computed at α=40 deg and δ=30 deg. Once again, the SWSWI effects for Earth are stronger than those for Mars.

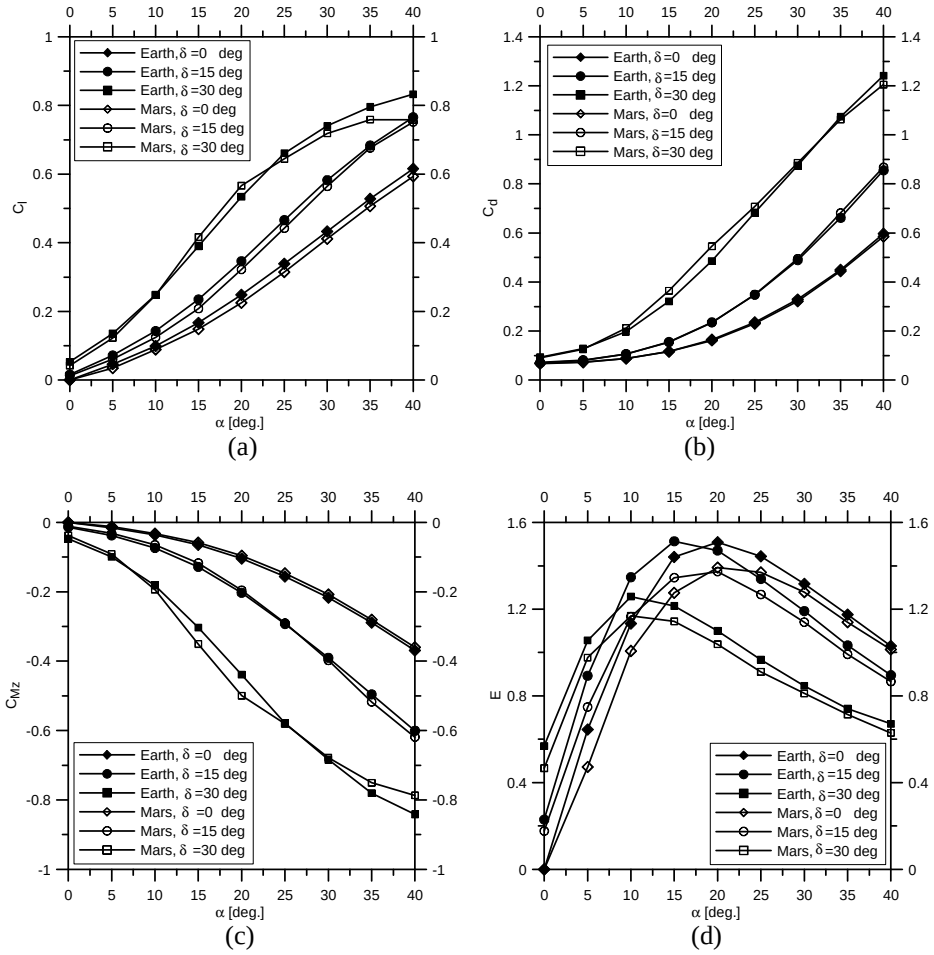

FIGURE 7. Profiles of lift (a), drag (b), pitching moment (c) coefficients and of aerodynamic efficiency (d) as functions of the angle of attack for Mars and Earth: h=65 km

TABLE 5. Comparison of the SWSWI effects for Mars and Earth: h=65 km, α=40 deg, δ=30 deg

	$\Delta C_l/C_l$	$\Delta C_d/C_d$	$\Delta C_{mz}/C_{mz}$	$\Delta E/E$
Mars	0.28	1.06	1.19	-0.38
Earth	0.35	1.08	1.28	-0.35

CONCLUSIONS AND FURTHER DEVELOPMENTS

The forthcoming manned exploration missions to Mars by means of complex geometry spacecrafts, as per lifting vehicles, stimulated the study of aerodynamic, hypersonic phenomena such as Shock Wave-Boundary Layer Interaction (SWBLI) and Shock Wave-Shock Wave Interaction (SWSWI) in Mars entry. The author already studied both interactions in Earth re-entry. Both the Earth and the Mars studies have been carried out computationally by means of a DSMC code (DS2V-4.5 64 bits).

The SWBLI effects have been evaluated in the altitude interval 55-70 km, considering an external shock wave generated by a 20 deg wedge, impinging onto a flat plate on which gas was flowing and therefore a boundary layer was present. The SWSWI effects have been evaluated at 65 km, considering a NACA-0010 airfoil in the range of angles of attack 0-40 deg and three flap angles of 0, 15 and 30 deg. SWSWI was generated by the interaction of the shock

wave on the airfoil leading edge with that stemming from the hinge position on the concave, lower surface of the same flapped airfoil.

Due to the higher values of the free stream dynamic pressure and of the energy flux for Earth, the influence of SWBLI on the resultant stress (f) or the resultant of pressure, normal and tangential stresses and on heat flux ($\dot{q}$) in Earth re-entry are higher than those in Mars entry. Also the SWSWI effects on the airfoil global aerodynamic coefficients and on the maximum values of f and $\dot{q}$ are higher for Earth. On the opposite, the SWSWI effects on the relative increment of f and of $\dot{q}$ are higher for Mars.

Further investigations will focus on SWSWI. 2-D and 3-D DSMC computations have been already scheduled and will be carried out taking into account other possible Earth re-entry and Mars entry trajectories of lifting vehicles provided with control aerodynamic surfaces. Moreover, the effects of the Edney's "type IV" SWSWI will be also computed and compared.

REFERENCES

1. G. Zuppardi and C. Boffa, "Effects of Rarefaction on the Shock Wave/Boundary Layer Interaction in Hypersonic Regime", Proceedings of the 28th International Symposium on Rarefied Gas Dynamics (RGD28), Zaragoza, Spain, 2012
2. G. Zuppardi, "Effects of Rarefaction on the Shock Wave/Shock Wave Interaction in Hypersonic Regime", Paper presented at the workshop DSMC13, Santa Fe, USA, 2013
3. G. Zuppardi, Advances in Aircraft and Spacecraft Science, **2**(1), 45-56, 2015
4. G. Zuppardi, D. Vangone, Advances in Aircraft and Spacecraft Science, **4**(5), 503-514, 2017
5. G. A. Bird, "Visual DSMC Program for Two-Dimensional Flows, the DS2V Program User's Guide, Ver. 4.5", G.A.B. Consulting Pty Ltd, Sidney, Australia, 2008.
6. J. D. Anderson, *Hypersonic and High Temperature Gas Dynamics* (McGraw-Hill International Editions, New York, USA, 1989
7. J. J. Bertin, *Hypersonic Aerothermodynamics* (AIAA Education Series, Washington, USA, 1994)
8. G. A. Bird, *Molecular Gas Dynamics and Direct Simulation Monte Carlo* (Clarendon Press, Oxford, United Kingdom, 1998
9. G. A. Bird, *The DSMC Method*, *Version 1.1* (Amazon, ISBS 9781492112907, Charleston, USA, 2013)
10. C. Shen, *Rarefied Gas Dynamic: Fundamentals, Simulations and Micro Flows* (Springer-Verlag, Berlin, Germany, 2005
11. G. A. Bird, "Sophisticated Versus Simple DSMC", Proceedings of the 25th International Symposium on Rarefied Gas Dynamics (RGD25), Saint Petersburg, Russia, 2006
12. G. A. Bird, M. A. Gallis, J. R. Torczynski and D. J. Rader, *Physics of Fluids*, **21**(1), DOI:10.1063/1.3067865, 2009
13. M. A. Gallis, J. R. Torczynski, D. J. Rader and G. A. Bird, *Journal of Computational Physics* **228**(12), 4532-4548, 2009
14. G. Zuppardi and R. Savino, "DSMC Aero-thermo-dynamic Analysis of a Deployable Capsule for Mars Atmosphere Entry", Paper presented at the workshop DSMC15, Kauai, Hawaii (USA), 2015
15. G. A. Bird, "The DS2V Program User's Guide Ver. 3.3", G.A.B. Consulting Pty Ltd, Sydney, Australia, 2005
16. G. Zuppardi, G. Visone, R. Votta and A. Schettino, *J. Aerosp. Eng.*, **225**(3), 247-258, 2011
17. J. N. Moss, "Rarefied Flows of Planetary Entry Capsules", Special course on "Capsule Aerothermodynamics", Rhode-Saint-Genèse, Belgium, May, AGARD-R-808, 95-129, 1995
18. R. D. Neumann, "Special Topics in Hypersonic Flow, in Aerodynamic Problems of Hypersonic Vehicles", AGARD LS 42, 1972